Journal of Southeast University (English Edition) Vol. 34, No. 3, pp. 386 - 393 Sept. 2018 ISSN 1003—7985

# Stability analysis of lead-vehicle control model in cooperative adaptive cruise control platoon within heterogeneous traffic flow

Gu Haiyan[1,2] Zhang Jian[1] Jin Peter J.[3] Ran Bin[1]

([1] School of Transportation, Southeast University, Nanjing 210096, China)

([2] College of Transportation Science & Engineering, Nanjing Tech University, Nanjing 210009, China)

([3] Department of Civil and Environmental Engineering, The State University of New Jersey, Piscataway, NJ 08854, USA)

**Abstract:** In order to analyze the stability impact of cooperative adaptive cruise control (CACC) platoon, an adaptive control model designed for the lead vehicle in a CACC platoon (LCACC model) in heterogeneous traffic flow with both CACC and manual vehicles is proposed. Considering the communication delay of a CACC platoon, a frequency-domain approach is taken to analyze the stability conditions of the novel lead-vehicle CACC model. Field trajectory data from the next-generation simulation (NGSIM) data is used as the initial condition. To account for car-following behaviors in reality, an intelligent driver model (IDM) is calibrated with the same NGSIM dataset from a previous study to model manual vehicles. The stability conditions of the proposed model are validated by the ring-road stability analysis. The ring-road test results indicate the potential of the LCACC model for improving the traffic flow stability impact of CACC platoons. Sensitivity analysis shows that the CACC fleet size has impact on the parameters of the LCACC model.

**Key words:** stability analysis; cooperative adaptive cruise control (CACC) platoon; lead-vehicle model; frequency-domain approach

**DOI:** 10.3969/j.issn.1003-7985.2018.03.015

Freeway traffic flow control requires mathematical models to describe the characteristics of traffic flow. These models must capture the essential character of the traffic flow behavior to develop the effective state estimation, filtering and control algorithms. Various categories of traffic flow models have been developed by researchers in the past to support simulation and control design[1-2]. The car following models[3] focus on the microscopic characteristics of traffic flow, such as lane-changing behavior, car-following behavior, and traffic trajectory.

Adaptive cruise control (ACC) systems, one type of driving-assistant system, aim to comfort drivers by releasing driving tasks and to benefit traffic efficiency and safety, have been developed for more than ten years and are even used on the market in some countries. The existing research work, based on microscopic simulations, has also proven that ACC systems can contribute to the stabilization, fuel economy and exhaust emissions of the corresponding traffic flow[4-7]. With the emergence of reliable vehicle-to-vehicle (V2V) communications, the next step in the development of ACC points is to cooperate with V2V communications to obtain more extensive and reliable information on vehicles.

The cooperative adaptive cruise control (CACC) system, which is an extension of the ACC system concept, is a new realization of longitudinal automated vehicle control. Compared with the ACC system, the CACC system can provide much more information about the surrounding vehicles through the vehicle-to-vehicle wireless communication mechanism. The impacts of CACC systems on traffic flow characteristics have recently been widely evaluated through microsimulation and experimental studies[8-11].

The focus of this study, however, is on the stability of heterogeneous traffic flow that contains CACC platoons and manual driving vehicles, based on the evaluation framework proposed in Ref. [12]. All the vehicles in the traffic flow can be sorted into two types, which are manual driving vehicles and CACC platoons. A novel lead-vehicle CACC (LCACC) model is used to simulate the car-following behavior of the lead vehicle of CACC platoon. A normal CACC model is used to describe CACC vehicles characteristics. Manual driving vehicles are modeled by the IDM.

## 1 Related Work

Two different criteria for stability that are central to the study of traffic flow problems should be considered: string stability and traffic flow stability. Some researchers have physically motivated and then mathematically defined the string stability and traffic flow stability and the difference between the two[13]. With the development of ACC/CACC, there are some impacts on the methods of

**Received** 2017-12-06, **Revised** 2018-02-20.

**Biographies:** Gu Haiyan (1988—), female, Ph. D. candidate; Zhang Jian (corresponding author), male, doctor, associate professor, zhangjian8seu@163.com.

**Foundation item:** The National High Technology Research and Development Program of China (863 Program) (No. 2011AA110405).

**Citation:** Gu Haiyan, Zhang Jian, Jin Peter J., et al. Stability analysis of lead-vehicle control models in cooperative adaptive cruise control platoon within heterogeneous traffic flow[J]. Journal of Southeast University (English Edition), 2018, 34(3): 389 - 393. DOI: 10.3969/j.issn.1003-7985.2018.03.015.

stability analysis.

### 1.1 Simulation method

A traffic simulation model MIXIC was developed in Ref. [14] to describe the impact of CACC on traffic performance, traffic safety, exhaust-gas emission, and noise emission. The results show an improvement in traffic stability and a slight increase in traffic-flow efficiency compared with that of the merging scenario without equipped vehicles[8]. The Newell model was used in simulation to analyze the influence of V2V on traffic flow string stability[15].

### 1.2 Analytical method

#### 1.2.1 A frequency-domain approach for string stability

For a constant velocity-independent intervehicle spacing, string stability cannot be guaranteed. The theoretical finding can be further validated by experiments conducted with two CACC-equipped vehicles. The string-stability characteristics of the CACC system are analyzed using a frequency-domain-based approach[16].

In Fig. 1, $G_i = G_i(s)$ represents the dynamics of the $i$-th vehicle; $K_i = K_i(s)$ is the corresponding ACC feedback controller; $F_i = F_i(s)$ is the feedforward filter; $D_i = D_i(s)$ is the communication delay; $s$ is the Laplace operator; and $h_{\mathrm{d},i}$ is the headway time. For clarity, the time dependency of the signals is omitted. The experimental results yield significant findings for CACC. With the relatively simple vehicular system and standard ACC algorithm, there have been significant improvements on the minimal headway time and string-stability characteristics[17]. Guo et al. [18] presented a systematic method that can guarantee string stability, achieve zero steady-state spacing error, and ensure a certain level of control performance at the same time.

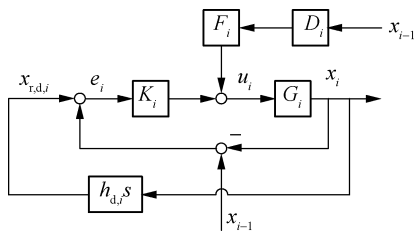


**Fig. 1** CACC control diagram

#### 1.2.2 Space error method for string stability

The string stability is defined as spacing errors, i.e., in a string-stable platoon, the spacing errors between vehicles are not amplified when propagating toward the tail of the platoon. $E_i$ is denoted as the spacing error between two adjacent vehicles. Then, the string stability implies that

$$\left\| \frac{E_{i+1}(s)}{E_i(s)} \right\|_\infty \leqslant 1 \tag{1}$$

where $E(s)$ is the Laplace transform of the spacing error. This definition is adopted by many researchers[19-20]. However, in the grand cooperative driving challenge (GCDC), string stability is defined using the vehicle accelerations[21]:

$$\left\| \frac{A_{i+1}(s)}{A_i(s)} \right\|_\infty \leqslant 1 \tag{2}$$

where $A(s)$ is the Laplace transform of the vehicle acceleration. Such a criterion is used to guarantee that the accelerations are not amplified upstream in the platoon.

#### 1.2.3 String stability for heterogeneous traffic

A longitudinal controller that uses the information exchanged via wireless communication with other cooperative vehicles to achieve string-stable platoon is developed[9]. An appropriate sensitivity function for heterogeneous traffic shown in Ref. [22] is

$$S_i(s) = \frac{X_i}{X_{i-1}} \qquad i = 2, 3, \ldots, m \tag{3}$$

where $m$ is the number of vehicles in the platoon and $X_i$ is the Laplace transforms of the location of vehicle $i$. If $X_i$ is the leading vehicle, then $X_i = S_i S_{i-1} \ldots S_2 S_1$, and a necessary condition to avoid amplification of oscillation is that

$$\| S_i \|_\infty = \sup_\omega | S_i(j\omega) | \leqslant 1 \qquad \forall i$$

Considering the switch to ACC, we obtain

$$S_i(s) = \frac{X_i}{X_{i-1}} = \frac{[k_1 + sk_2 + s^2 K_3(s)]\, G(s)}{1 + [k_1(1 + sh) + sk_2]\, G(s)} \tag{4}$$

#### 1.2.4 Linear stability for heterogeneous traffic flow

Ngoduy[23] conducted a linear stability analysis to find the stability threshold of heterogeneous traffic flow using car-following models. The effect of intelligent vehicles on heterogeneous (or multiclass) traffic flow instabilities is analyzed. The results show how intelligent vehicle percentages affect the stability of multiclass traffic flow. This paper extends to the multiclass time-continuous intelligent driver model with time delays[24]. Most current analytical research has only relied on single-class traffic flow dynamics.

## 2 Methodology

As discussed in Ref. [12], we consider a platoon of $n + m$ vehicles traveling in a single lane as shown in Fig. 2. The preceding $m$ vehicles are not equipped with CACC vehicles and are assumed to be human-driven. The leading vehicle implements acceleration using acceleration signals received from preceding vehicles through radar. We assume that the leading vehicle can only sense the velocity and distance information from one preceding vehicle assuming no communication between leading vehicles and manually driven vehicles. CACC vehicles share the prevailing states of vehicles among CACC platoons such as distance, velocity and acceleration.

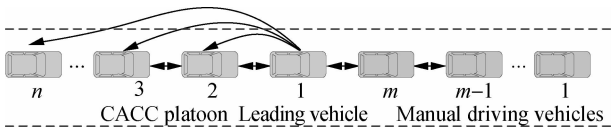


**Fig. 2** A mixed manual and CACC vehicle platoon

### 2.1 LCACC and CACC model equation

Microscopic traffic flow models describe the motion of individual vehicle $n$ in response to its leading vehicle $n-1$. In this paper, we use the LCACC model[12] for the leading vehicle of the CACC platoon:

$$a_{\mathrm{L}}(t) = \alpha(k_1(v_{\mathrm{p}}(t) - v_{\mathrm{L}}(t)) + k_2(c_L(t) - c_{1,\mathrm{des}}(t))) + \beta\frac{\sum_{i=2}^{N}[k_1(v_{\mathrm{L}}(t) - v_i(t)) + k_2(c_i(t) - c_{i,\mathrm{des}}(t))]}{(N-1)k_0}$$
$$\alpha + \beta = 1 \tag{5}$$

where $N$ is the number of CACC vehicles; $v_{\mathrm{p}}(t)$ is the velocity of the manual driving vehicle in front of the leading vehicle; $k_0$, $k_1$, $k_2$ are the positive parameters; and $\alpha$, $\beta$ are the contribution percentages of forward and backward; $c_{i,\mathrm{des}}(t)$ is the designed clearance between vehicle $i$ and the preceding vehicle; $c_i(t)$ is the actual clearance between vehicle $i$ and the preceding vehicle.

For the rest of the vehicles in CACC platoon, the following CACC model is used[25]:

$$a_n(t) = k_0 a_0(t) + k_1(v_{n-1}(t) - v_n(t)) + k_2(c_n(t) - c_{n,\mathrm{des}}(t)) \qquad d_2 \leqslant a_n(t) \leqslant a_{\max} \tag{6}$$

where $a_{\max}$ is the maximum allowed acceleration and $d_2$ is the braking capability of following vehicles. The vehicle spacing $v_n(t)$ is the velocity of vehicle $n$ at time $t$.

$$\left.\begin{aligned} c_{\mathrm{d}}(t) &= \max(c_{\mathrm{safe}}(t), c_{0.5\mathrm{s}}(t), c_{\min}) \\ c_{\mathrm{safe}}(t) &= \frac{v_1^2(t)}{2}\left(\frac{1}{d_2} - \frac{1}{d_1}\right) + \delta v_1^2(t) \\ c_{0.5\mathrm{s}}(t) &= 0.5 v_2^2(t) \end{aligned}\right\} \tag{7}$$

where $c_{\mathrm{d}}$, $c_{\mathrm{safe}}$, $c_{0.5\mathrm{s}}$ are desired, safety, and $t$-second-time-gap spacing, respectively; $\delta$ is the communication delay; $d_1$ is the braking capability of the preceding vehicle; and $d_2$ is the braking capability of the following vehicle.

The intelligent driver model (IDM)[26] is also introduced to control the ACC/CACC vehicles. The IDM acceleration is given by

$$\left.\begin{aligned} a_n(t) &= \alpha\left[1 - \left(\frac{v}{v_0}\right)^4 - \left(\frac{s^*(v, \Delta v)}{s}\right)^2\right] \\ s^*(v, \Delta v) &= s_0 + vT + \left(\frac{v, \Delta v}{2\sqrt{ab}}\right) \end{aligned}\right\} \tag{8}$$

where $s_0$ is the minimum distance in congested traffic flow; $T$ is a constant safe time gap; $v_0$ is the desired speed on a free road; $v$ is the actual speed on a free road; $a$ is the maximum acceleration; and $b$ is the comfortable deceleration; $s$ is the spacing between vehicle $(n-1)$ and vehicle $n$ at time $t$; $\Delta v$ is the velocity difference between vehicle $(n-1)$ and vehicle $n$ at time $t$; and $\alpha$ is a constant.

### 2.2 CACC control structure

Consider a string of heterogeneous vehicles, as depicted in Fig. 3, where $x_{\mathrm{r},i}(t)$, $\dot{x}_{\mathrm{r},i}(t)$, $\ddot{x}_{\mathrm{r},i}(t)$ and $l_i$ are the relative position, the relative velocity, the acceleration, and the length of vehicle $i$, respectively. Through the wireless communication, the acceleration of the leading vehicle of CACC platoon $\ddot{x}_{\mathrm{L}}(t)$ is available.

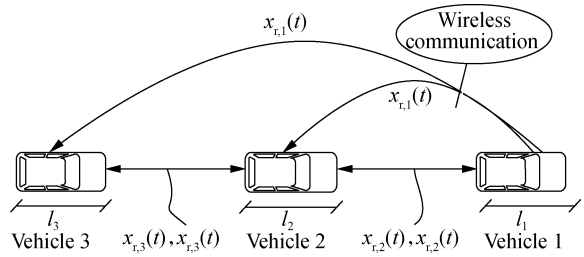


**Fig. 3** Schematic of a platoon of CACC vehicles

In Fig. 4, $G_i = G_i(s)$ represents the dynamic of the $i$-th vehicle; $K_i = K_i(s)$ is the corresponding ACC feedback controller; $F_i = F_i(s)$ is the feedforward filter; $D_i = D_i(s)$ is the communication delay; and $h_{\mathrm{d},i}$ is the time headway. $a_i(t)$ is the desired acceleration $\ddot{x}_{\mathrm{d},i}(t)$. $x_{\mathrm{r},i}(t)$ is the actual distance, and $x_{\mathrm{r,d},i}(t)$ is the desired distance. $x_i(t)$ is the actual location of ith vehicle. $X_i(s)$ are the Laplace transforms of the input $x_i(t)$. $V_i(s)$ are the Laplace transforms of the input $v_i(t)$. $E_i(s)$ are the Laplace transforms of the input $e_i(t)$. A feedback controller controls the spacing error.

$$e_i(t) = x_{\mathrm{r},i}(t) - x_{\mathrm{r,d},i}(t) \tag{9}$$

The relationship between time headway and desired distance is

$$x_{\mathrm{r,d},i}(t) = h_{\mathrm{d},i}\dot{x}_i(t) \tag{10}$$

The acceleration of the preceding vehicle is used as a feedforward control signal through a feedforward filter $F_i(s)$. The acceleration is obtained through wireless communication, which includes a communication delay $D_i(s)$. The resulting control structure is schematically depicted in Fig. 4. In this paper, the focus is not on a single CACC vehicle but on a CACC platoon. The control structure is shown in Fig. 5.

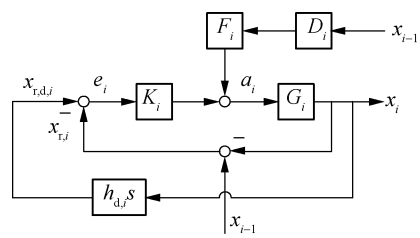


**Fig. 4** CACC control structure[16]

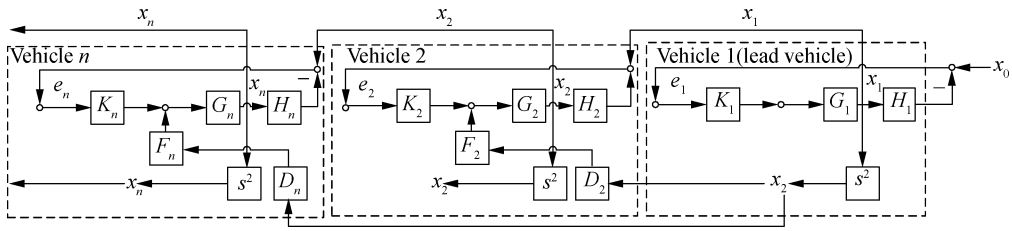


**Fig. 5** CACC platoon control structure

### 2.3 String stability

The delay is represented by a constant delay time $\theta_i$, yielding

$$L(\ddot{x}_{i-1}(t-\theta_i)) = D_i(s)s^2X_{i-1}(s) \tag{11}$$

where $D_i(s) = e^{-\theta s}$, for $i>1$, and $L(\cdot)$ denotes the Laplace transformation. The design of the feedforward filter is based on a zero-error condition, where the Laplace transform of the error $e_i(t)$ is defined as

$$L(e_i(t)) = \frac{1-H_i(s)G_i(s)F_i(s)D_i(s)s^2}{1+H_i(s)G_i(s)K_i(s)}L(x_{i-1}(t)) \qquad i>1 \tag{12}$$

Consider the CACC control structure[16] shown in Fig. 4. Coupling some of these control structures yields the control structure for a platoon of vehicles, as shown in Fig. 5, where the inner and the outer control loops are merged using the definition of $H_i(s)$.

$$H_i(s) = 1 + h_{d,i}s \qquad i>1 \tag{13}$$

The first vehicle in the platoon ($i=1$) is assumed to follow a given time-varying reference position $x_0(t)$ using radar measurements. The other vehicles in the platoon ($i>1$) use both radar and wireless communication.

The Laplace transforms of input are defined as $L(x_0(t)) = X_0(s)$, and the signals are defined as $v_i(t)$, $x_i(t)$, $e_i(t)$. $L(v_i(t)) = V_i(s)$, $L(x_i(t)) = X_i(s)$, and $L(e_i(t)) = E_i(s)$. We define the following string stability transfer functions:

$$\zeta'_{\Lambda,n}(s) = \frac{\Lambda_n(s)}{\Lambda_1(s)} = \frac{\Lambda_n(s)}{X_0(s)}\left(\frac{\Lambda_1(s)}{X_0(s)}\right)^{-1} \qquad n>1 \tag{14}$$

where $n$ denotes the last vehicle in a platoon of vehicles. The magnitude of the string-stability transfer function $\zeta'_{\Lambda,n}(s)$ is a measure of the amplification of oscillations upstream a platoon. Hence, since string stability is defined as the damping of the magnitude of oscillations upstream from a platoon, a necessary condition for string stability is[27-28]

$$\| \zeta'_{\Lambda,n}(jw) \|_\infty \leqslant 1 \qquad n>1 \tag{15}$$

where $\| g \|_\infty$ denotes the maximum amplitude for all $\omega$.

$$\| \zeta'_{\Lambda,n}(jw) \|_\infty = 1 \qquad n>1, \omega>0 \tag{16}$$

For heterogeneous traffic, i. e., vehicles with potentially different characteristics and dynamics, this condition requires a complicated communication mechanism. In this paper, for the communication in the platoon, since only the leading vehicle is considered, all the vehicles in CACC platoon should satisfy the string-stability transfer functions in (14). In the rest of this paper, the sufficient condition (16) is considered a necessary condition for string stability.

$$\zeta_{a,i} = \frac{a_i}{a_{i-1}} = S_i(F_iD_is^2 + K_i)G_1 \qquad i>1 \tag{17}$$

$$\zeta_{X,i} = \frac{X_i}{X_{i-1}} = S_i(F_iD_is^2 + K_i)G_i \qquad i>1 \tag{18}$$

$$\zeta_{E,i} = \frac{E_i}{E_{i-1}} = \begin{cases} S_2(1-\Xi_2)G_1K_1 & i=2 \\ \dfrac{S_i(1-\Xi_i)}{S_{i-1}(1-\Xi_{i-1})}\dfrac{X_{i-1}}{X_{i-2}} & i>2 \end{cases} \tag{19}$$

where $\Xi_i(s) = H_i(s)G_i(s)F_i(s)D_i(s)s^2$, $S_i(s) = (1+H_i(s)G_i(s)K_i(s))^{-1}$.

Substituting the feedforward filter $F_i(s)$ in (18) yields

$$F_i(s) = (H_i(s)G_i(s)s^2)^{-1} \qquad i>1 \tag{20}$$

$$\zeta_{X,i}(s) = \frac{X_i}{X_{i-1}} = \frac{D_i(s)+H_i(s)G_i(s)K_i(s)}{H_i(s)(1+H_i(s)G_i(s)K_i(s))} \qquad i>1 \tag{21}$$

**Case 1** No communication delay. According to the assumption, there is no communication delay between the following vehicles in the CACC platoon, $\theta_i = 0$ s, $D_i = 1$, Eq. (21) can be simplified as

$$\zeta_{X,i}(s) = \frac{X_i}{X_{i-1}} = \frac{1}{H_i(s)} \qquad i>1 \tag{22}$$

For any time headway $h_{d,i}s>0$,

$$H_i(s) = 1 + h_{d,i}s > 1, \quad \zeta_{X,i}(s) = \frac{X_i}{X_{i-1}} = \frac{1}{H_i(s)} < 1 \tag{23}$$

Hence, for the time headway $h_{d,i}>0$ s, the string stability condition (18) is always fulfilled.

**Case 2** Communication delay $\theta_i>0$ s. The $\theta_i$ values ranged from 0.3 to 0.6 s is used between the leading vehicle and the following vehicles based on prior research. The external feedforward of the lead vehicle in a CACC platoon is ignored. First, by considering the engine time constant, we have the dynamics of the $n$-th vehicle as

$$\tau_n \dot{a}_n + a_n = a_n^{\mathrm{des}} \tag{24}$$

where $\tau_n$ is the response time of the $n$-th vehicle; $a_n$ and $a_n^{\mathrm{des}}$ are the real acceleration and desired acceleration of the $n$-th vehicle, respectively. In this study, we use a linear CACC control model defined in Eq. (24),

$$a_n^{\mathrm{des}} = k_0 a_1 + k_1(v_1 - v_n) + k_2(s_n - s_{\mathrm{des}}) \tag{25}$$

$$\tau_n \ddot{a}_n + \dot{a}_n = k_0 a_1 + k_1(v_1 - v_n) + k_2(s_n - d_{\mathrm{des}}) \tag{26}$$

By differentiating both sides of Eq. (26), we obtain

$$\tau_n \dddot{a}_n + \ddot{a}_n = k_0 \dddot{x}_1 + k_1(\ddot{x}_1 - \ddot{x}_n) + k_2(\dot{x}_{n-1} - \dot{x}_n) \tag{27}$$

By taking the Laplace transformation on both sides of (27), we can obtain the relationship between vehicle $n$ and $n-1$ as

$$\left.\begin{aligned} &(\tau_n s^3 + s^2 + k_1 s + k_2) V_n = (k_0 s^2 + k_1 s) V_1 + k_2 V_{n-1} \\ &V_n = \frac{(k_0 s^2 + k_1 s) V_1 + k_2 V_{n-1}}{\tau_n s^3 + s^2 + k_1 s + k_2} \end{aligned}\right\} \tag{28}$$

To achieve the string stability, spacing error must be smaller than or equal to the spacing error input. For a CACC vehicle platoon, the string stability is defined as

$$\left\| \frac{V_n(s)}{V_{n-1}(s)} \right\|_\infty \leqslant 1 \tag{29}$$

According to the assumptions, the delay only exists between the leading vehicle and the following vehicle. All the following vehicles will make a decision at the same time. In this way, we only consider the situation when $n = 2$.

$$\left\| \frac{V_1(s)}{V_2(s)} \right\|_\infty = \left\| \frac{k_0 s^2 + k_1 s + k_2}{\tau_n s^3 + s^2 + k_1 s + k_2} \right\|_\infty \leqslant 1 \tag{30}$$

Eq. (30) can be simplified as

$$\left\| \frac{V_n(s)}{V_{n-1}(s)} \right\|_\infty = \sqrt{\frac{p}{q}} \tag{31}$$

where

$$\begin{aligned} p &= (k_2 - k_0\omega^2)^2 + (k_1\omega)^2 = k_0^2\omega^4 + (k_1^2 - 2k_0k_2)\omega^2 + k_2^2 \\ q &= (k_2 - \omega^2)^2 + (-\tau_n\omega^3 + k_1\omega)^2 = \tau_n^2\omega^6 + \\ &\quad (1 - 2k_1\tau_n)\omega^4 + (k_1^2 - 2k_2)\omega^2 + k_2^2 \end{aligned}$$

$\| V_n(s)/V_{n-1}(s) \|_\infty \leqslant 1$ can be satisfied when $p < q$, that is, $q - p > 0$.

$$\begin{aligned} q - p &= [\tau_n^2\omega^6 + (1 - 2k_1\tau_n)\omega^4 + (k_1^2 - 2k_2)\omega^2 + k_2^2] - \\ &\quad [k_0^2\omega^4 + (k_1^2 - 2k_0k_2)\omega^2 + k_2^2] = \\ &\quad \omega^2(\tau_n^2\omega^4 + (1 - 2k_1\tau_n - k_0^2)\omega^2 + 2k_0k_2 - 2k_2) \end{aligned} \tag{32}$$

In the selected CACC model, all parameters $k_0$, $k_1$, $k_2$ are greater than or equal to zero. Four different situations are considered based on the values of $k_0$, $k_1$, $k_2$. Tab. 1 summarizes the value range of $\tau_n$ with different values of parameters $k_0$, $k_1$, $k_2$ ensuring stability, where $\tau_n \in (\tau^-, \tau^+)$.

**Tab. 1** Stability condition with different values of parameters in the LCACC model

| $k_0$ | $k_1$ | $k_2$ | $\tau^-$ | $\tau^+$ |
|---|---|---|---|---|
| 0 | >0 | 0 | 0 | $\max\left\{\frac{x_{n-1}(t) - x_n(t) - L_{n-1} - d_{\mathrm{safe}}}{v_n(t) - v_{n-1}(t)}, \tau_0, \frac{1}{2k_1}\right\}$ |
| 1 | 0 | >0 | 0 | $\max\left\{\frac{x_{n-1}(t) - x_n(t) - L_{n-1} - d_{\mathrm{safe}}}{v_n(t) - v_{n-1}(t)}, \tau_0\right\}$ |
| >0 | >0 | 0 | $\frac{1 - k_0^2}{2k_1}$ | $\max\left\{\frac{x_{n-1}(t) - x_n(t) - L_{n-1} - d_{\mathrm{safe}}}{v_n(t) - v_{n-1}(t)}, \tau_0\right\}$ |
| >1 | >0 | >0 | $\frac{(k_0^2 - 1)k_1}{4k_0k_2 - 4k_2 - 2k_1^2} + \frac{(k_0^2 - 1)\sqrt{2k_0k_2 - 2k_2}}{4k_0k_2 - 4k_2 - 2k_1^2}$ | $\max\left\{\frac{x_{n-1}(t) - x_n(t) - L_{n-1} - d_{\mathrm{safe}}}{v_n(t) - v_{n-1}(t)}, \tau_0\right\}$ |

## 3 Experimental Results and Analysis

### 3.1 Initial input data design

The ring road is closed by making the back bumper location of the first and the 35th vehicle the same point in the initial state. The inner lane data is used to obtain a real-world "pipeline" scenario close to the ring-road environment. Secondly, the IDM model parameters calibrated based on the same dataset in a previous study are used for modeling manual vehicles. The CACC and LCACC models are applied continuously for 1 000 time intervals to evaluate their stability patterns. The initial speeds of all vehicles are approximately the same (32.9 km/h), and the clearance between any two vehicles is the same. Additionally, the acceleration is zero for all the vehicles. At the time $t = 0$ s, a small disturbance will be added to one vehicle in the stable traffic flow.

### 3.2 Ring-road test of string stability

Two experiments are performed with different model parameter settings:

1) A CACC platoon using LCACC. We use the LCACC model to simulate the characteristic of lead vehicle of the CACC platoon, the normal CACC model for the rest of the CACC vehicle platoon, and the IDM model for manual vehicles.

2) A CACC vehicle platoon without using LCACC (CACC). All the CACC vehicles are simulated by a normal CACC model, and the manual vehicles are modeled with IDM.

Fig. 6 and Fig. 7 exhibit the stability characteristics of different evaluation scenarios. The $X$-axis represents the

simulation time step (0 to 1 000 time steps), the *y*-axis represents the ring-road length (0 to 0.6 km). Color coding displays the velocity (0 to 65 km/h, 18.06 m/s), and 5, 10, 20 are the CACC fleet size. The individual points in each diagram are the trajectory points of vehicles traveling in the ring-road. The color of each point is determined based on the velocity, with blue indicating the free flow and red indicating slow-moving or stopping points. Fig. 6 and Fig. 7 confirm the numerical results, indicating string stability both in the case of CACC and LCACC with a desired headway time. With the increase in the CACC fleet size, the string stability condition is not always satisfied. For a fixed time headway, the LCACC model is more stable than the CACC model. When the

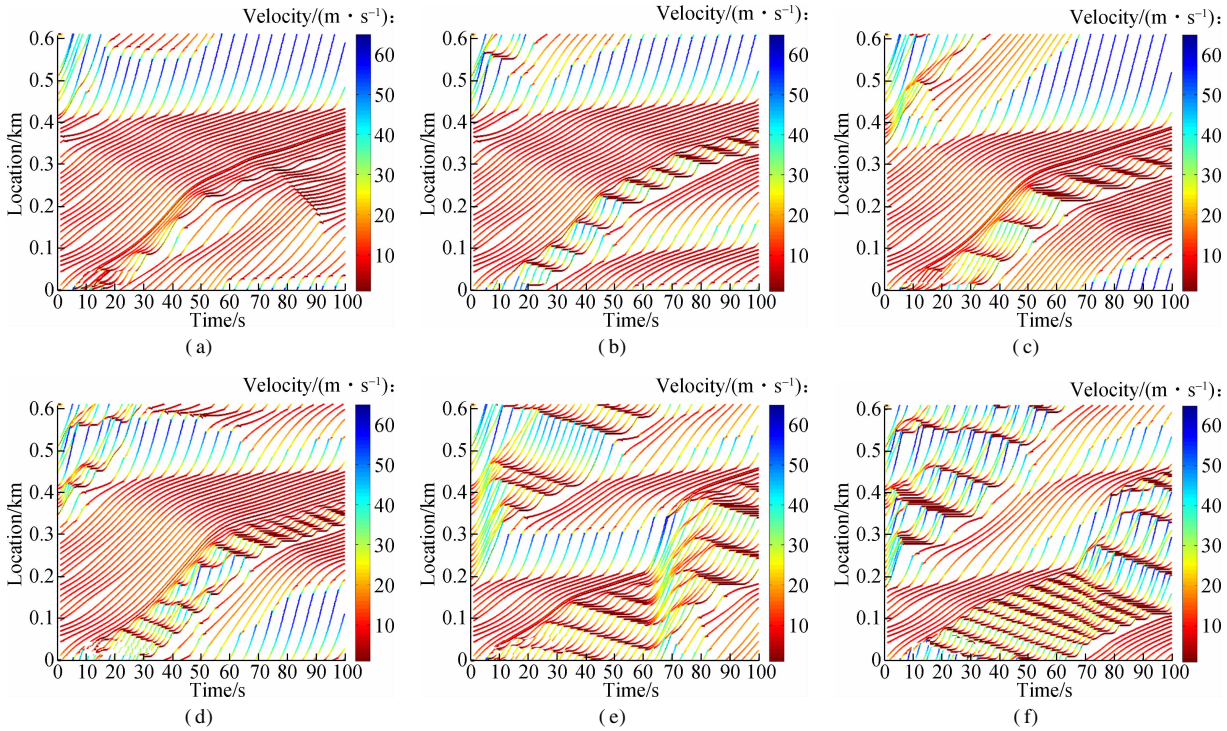


**Fig. 6** Ring-road stability test results for designed time headway $h_{d,i} = 0.5$ s. (a) LCACC-5; (b) CACC-5; (c) LACCC-10; (d) CACC-10; (e) LCACC-20; (f) CACC-20

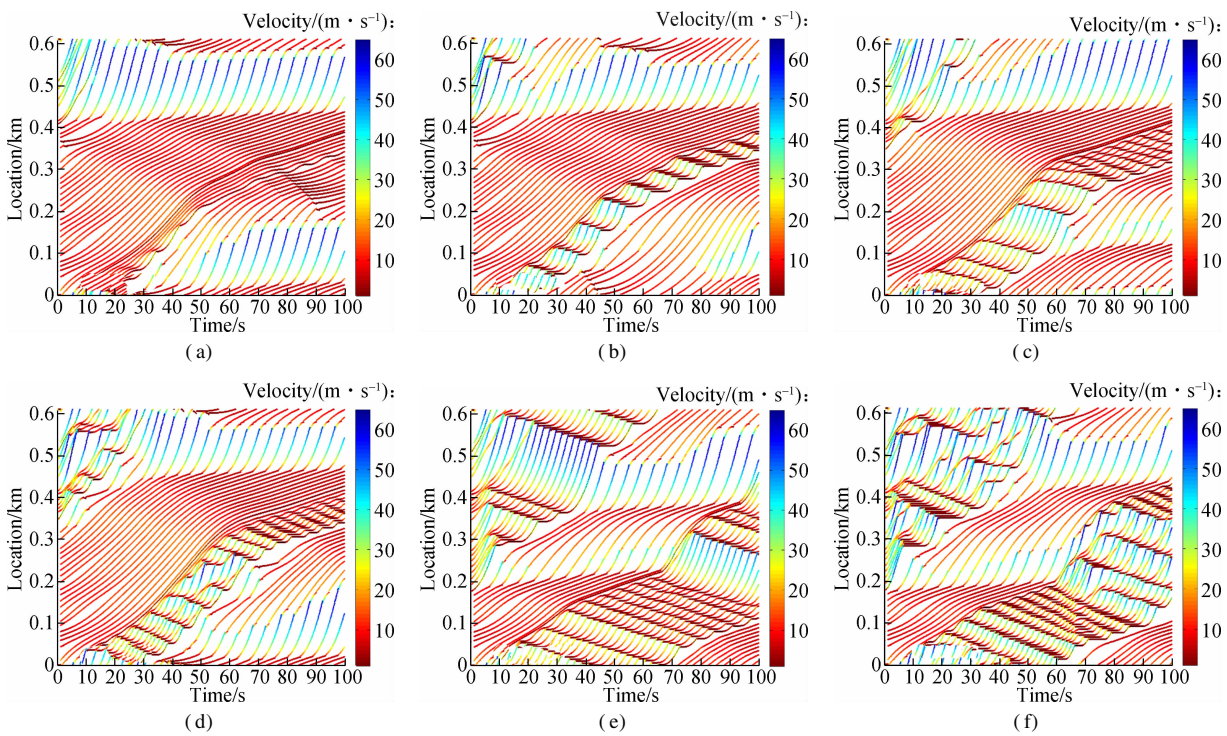


**Fig. 7** Ring-road stability test results for designed time headway $h_{d,i} = 1.5$ s. (a) LCACC-5; (b) CACC-5; (c) LACCC-10; (d) CACC-10; (e) LCACC-20; (f) CACC-20

time headway is smaller than 0.5 s, the string stability condition is not satisfied for both LCACC and CACC scenarios.

### 3.3 Stability experiment with NGSIM data

This study used vehicle trajectory data collected in a southbound direction of US Highway 101 (Hollywood Freeway) in Los Angeles, California on June 15th, 2005, from the NGSIM project. The data collection time period is 45 min, between 07:50 and 08:35, during the morning peak hours with a temporal resolution of 0.1 s. First, the states of the last 35 vehicles on Lane 1 at 08:30 during peak hour congestion are used as the initial traffic states on the ring-road. This information establishes a realistic "perturbation pattern" of heterogeneous acceleration, velocity, and spacing for stability analysis. The ring road is closed by making the back bumper location of the first and the 35th vehicle the same point at the initial state.

Tab. 2 depicts the comparison results for LCACC, CACC, and manual driving under different CACC fleet sizes. The first noticeable pattern is that car-following models, although calibrated from the same NGSIM dataset and started from the same initial condition, can exhibit significantly different stability results. The size of the congestion area (CA) is also shown in the table and used as a car-following stability indicator where larger values mean higher congestion (instability). CA is obtained by the total size of all the vehicles in 10 s by a 30.4 m range, which has an average vehicle velocity below 30 km/h. The stability can also be evaluated by inspecting the frequency of congestion bands.

**Tab. 2** Congestion area for mixed traffic flow condition

| Lead-vehicle model | CACC fleet size | | |
|---|---|---|---|
| | 5 | 15 | 20 |
| LCACC model | 45.12 | 48.16 | 45.42 |
| CACC model | 51.82 | 51.51 | 48.16 |

In general, the string stability of vehicles with CACC and LCACC platoons is better than that of all manual vehicles, with significantly reduced CA values shown in Tab. 2. With the increase in the CACC fleet size, the trend of the CA value decreases. The heavy low-frequency congestion is reduced to light congestion with increased frequency. Meanwhile, LCACC platoons also exhibit a better capability of stabilizing traffic flow than regular CACC platoons. Furthermore, the increase in the CACC fleet sizes, in general, results in the increased traffic stability.

## 4 Conclusions

1) If there is no communication delay, the CACC platoon will always satisfy the string stability condition. If a communication delay exists, the stability conditions are related to different values of parameters $k_0$, $k$, and $k_2$.

2) With the sensing and communication delay, more similar to real-life CACC platoons, the LCACC model can enable small vehicle spacing while maintaining string stability better than that of the CACC model.

3) For the LCACC model, the increase in the CACC fleet size will lead to better string stability.

4) The experimental results show a significant improvement on the minimal headway time using the LCACC model.

## References

[1] Darbha S, Rajagopal K R. Intelligent cruise control systems and traffic flow stability[J]. *Transportation Research Part C: Emerging Technologies*, 1999, **7**(6): 329 − 352. DOI: 10.1016/S0968 − 090X(99)00024 − 8.

[2] Pipes L A. An operational analysis of traffic dynamics [J]. *Journal of Applied Physics*, 1953, **24**(3): 274 − 281. DOI: 10.1063/1.1721265.

[3] Lakouari N, Bentaleb K, Ez-Zahraouy H, et al. Correlation velocities in heterogeneous bidirectional cellular automata traffic flow[J]. *Physica A: Statistical Mechanics and Its Applications*, 2015, **439**: 132 − 141. DOI: 10.1016/j.physa.2015.07.024.

[4] Li Y, Wang H, Wang W, et al. Evaluation of the impacts of cooperative adaptive cruise control onreducing rear-end collision risks on freeways[J]. *School Accident Analysis and Prevention*, 2017, **98**: 87 − 95. DOI: 10.1016/j.aap.2016.09.015.

[5] Kesting A, Treiber M, Schönhof M, et al. Adaptive cruise control design for active congestion avoidance[J]. *Transportation Research Part C: Emerging Technologies*, 2008, **16**(6): 668 − 683. DOI: 10.1016/j.trc.2007.12.004.

[6] Liu F X, Cheng R J, Ge H X, et al. An improved car-following model considering the influence of optimal velocity for leading vehicle[J]. *Nonlinear Dynamics*, 2016, **85**(3): 1469 − 1478. DOI: 10.1007/s11071-016-2772-7.

[7] Zhou T, Sun D H, Kang Y R, et al. A new car-following model with consideration of the prevision driving behavior [J]. *Communications in Nonlinear Science and Numerical Simulation*, 2014, **19**(10): 3820 − 3826. DOI: 10.1016/j.cnsns.2014.03.012.

[8] van Arem B, van Driel C J G, Visser R. The impact of cooperative adaptive cruise control on traffic-flow characteristics[J]. *IEEE Transactions on Intelligent Transportation Systems*, 2006, **7**(4): 429 − 436. DOI: 10.1109/tits.2006.884615.

[9] Lidström K, Sjöberg K, Holmberg U, et al. A modular CACC system integration and design[J]. *IEEE Transactions on Intelligent Transportation Systems*, 2012, **13**(3): 1050 − 1061. DOI: 10.1109/tits.2012.2204877.

[10] Milanés V, Shladover S E. Modeling cooperative and autonomous adaptive cruise control dynamic responses using experimental data[J]. *Transportation Research Part C*, 2014, **48**: 285 − 300. DOI: 10.1016/j.trc.2014.09.001.

[11] Yu S W, Shi Z K. An extended car-following model at signalized intersections[J]. *Physica A: Statistical Mechanics and Its Applications*, 2014, **407**: 152 − 159. DOI: 10.1016/j.physa.2014.03.081.

[12] Gu H Y, Jin P J, Wan X, et al. A leading vehicle model

for comfortable acceleration among cooperative adaptive cruise control (CACC) vehicle platoons[C]//*Transportation Research Board* 94*th Annual Meeting*. Washington, DC, USA, 2014: 5215 - 5232.

[13] Darbha S, Rajagopal K R. Intelligent cruise control systems and traffic flow stability[J]. *Transportation Research Part C: Emerging Technologies*, 1999, **7**(6): 329 - 352. DOI: 10.1016/S0968 - 090X(99)00024 - 8.

[14] van Arem B, de Vos A P, Vanderschuren M. The microscopic traffic simulation model MIXIC 1.3[R]. Washington, DC, USA: TRID, 1997.

[15] Hua X D, Wang W, Wang H. A car-following model with the consideration of vehicle-to-vehicle communication technology[J]. *Acta Physica Sinica*, 2016, **65**(1): 010502-1 - 010502-12.

[16] Zheng L. Detailed string stability analysis for bi-directional optimal velocity model[J]. *Journal of Central South University*, 2015, **22**(4): 1563 - 1573. DOI: 10.1007/s11771-015-2673-9.

[17] Naus G J L, Vugts R P A, Ploeg J, et al. String-stable CACC design and experimental validation: A frequency-domain approach[J]. *IEEE Transactions on Vehicular Technology*, 2010, **59**(9): 4268 - 4279. DOI: 10.1109/tvt.2010.2076320.

[18] Guo G, Yue W. Autonomous platoon control allowing range-limited sensors[J]. *IEEE Transactions on Vehicular Technology*, 2012, **61**(7): 2901 - 2912. DOI: 10.1109/tvt.2012.2203362.

[19] Seiler P, Pant A, Hedrick K. Disturbance propagation in vehicle strings[J]. *IEEE Transactions on Automatic Control*, 2004, **49**(10): 1835 - 1841. DOI: 10.1109/tac.2004.835586.

[20] Shaw E, Hedrick J K. Controller design for string-stable heteroge-neous vehicle strings[C]// 46*th IEEE Conference on Decision and Control*. New Orleans, LA, USA, 2008: 2868 - 2875. DOI: 10.1109/CDC.2007.4435011.

[21] Kianfar R, Augusto B, Ebadighajari A, et al. Design and experimental validation of a cooperative driving system in the grand cooperative driving challenge[J]. *IEEE Transactions on Intelligent Transportation Systems*, 2012, **13**(3): 994 - 1007. DOI: 10.1109/tits.2012.2186513.

[22] Naus G, Vugts R, Ploeg J, et al. Towards on-the-road implementation of cooperative adaptive cruise control[C]//16*th ITS World Congress and Exhibition on Intelligent Transport Systems and Services*. Stockholm, Sweden, 2009, **58**(8): 6145 - 6150.

[23] Ngoduy D. Analytical studies on the instabilities of heterogeneous intelligent traffic flow[J]. *Communications in Nonlinear Science and Numerical Simulation*, 2013, **18**(10): 2699 - 2706. DOI: 10.1016/j.cnsns.2013.02.018.

[24] Orosz G, Wilson R E, Stépán G. Traffic jams: Dynamics and control[J]. *Philosophical Transactions of the Royal Society A: Mathematical Physical & Engineering Sciences*, 2010, **368**(1928): 4455 - 4479.

[25] Shladover S, Vanderwerf J, Miller M A, et al. Development and performance evaluation of AVCSS deployment sequences to advance from today's driving environment to full automation[J]. *Inorganic Chemistry*, 2001, **46**(1): 93 - 102.

[26] Treiber M, Hennecke A, Helbing D. Congested traffic states in empirical observations and microscopic simulations[J]. *Physical Review E*, 2000, **62**(2): 1805 - 1824. DOI: 10.1103/physreve.62.1805.

[27] Sheikholeslam S, Desoer C A. Longitudinal control of a platoon of vehicles with no communication of lead vehicle information: A system level study[J]. *IEEE Transactions on Vehicular Technology*, 1993, **42**(4): 546 - 554. DOI: 10.1109/25.260756.

[28] Liang C Y, Peng H. String stability analysis of adaptive cruise controlled vehicles[J]. *JSME International Journal Series C*, 2000, **43**(3): 671 - 677. DOI: 10.1299/jsmec.43.671.

# 混合交通流中协同式自适应车组引导车控制模型稳定性分析

顾海燕[1,2] 张 健[1] 金 璟[3] 冉 斌[1]

([1]东南大学交通学院, 南京 210096)

([2]南京工业大学交通运输工程学院, 南京 210009)

([3] Department of Civil and Environmental Engineering, The State University of New Jersey, Piscataway, NJ 08854, USA)

**摘要**:为了分析协同式自适应巡航控制(CACC)车组的稳定性影响,构建了混合交通流条件下协同式自适应巡航控制车辆组引导车模型(LCACC).考虑协同式自适应控制车组间的信息交互延误,采用频域变换的方法来推理引导车模型的稳定性边界条件.将美国 NGSIM 数据库轨迹数据作为初始输入,根据先前研究成果,采用 IDM 模型模拟混合交通流中人工驾驶车辆的驾驶行为,运用环道测试的方法来验证引导车模型的稳定性.环道测试结果表明,LCACC 模型在改善协同式自适应车组的稳定性方面有一定的优越性,敏感性分析显示 CACC 车组的大小对 LCACC 模型参数产生影响.

**关键词**:稳定性分析;协同式自适应巡航车队;引导车模型;频域变换法

**中图分类号**:U491